Study on Sb-based Alloy and Compound Powder as Lithium Ion Battery Anode Materials

Chengxue Lv, Hangjie Li, Ding Xu and Ruiqin Yang*

Zhejiang Provincial Key Lab. for Chem. & Bio. Processing Technology of Farm Products, School of Biological and Chemical Engineering, Zhejiang University of Science & Technology, Hangzhou, China

e-mail: yruiqin@163.com

Keywords: SbFe and Sb_2Fe alloys; Sb-Ge metal composite powder; Lithium ion battery; Anode materials.

Abstract. The $SbFeO_3$ was reduced to obtain the SbFe and Sb_2Fe alloys, and the $SbGeO_{3.5}$ was reduced to obtain the Sb-Ge metal composite powder. The simulation lithium ion battery was prepared by using the SbFe and Sb_2Fe alloys or the Sb-Ge metal composite powder as anode material. The analysis of the XRD and the SEM for the SbFe and Sb_2Fe alloys and the Sb-Ge metal composite powder were completed, and the electrochemical properties of the simulation battery were characterized. The results indicate that the first discharge capacity and charge capacity were 510mAh/g and 475mAh/g, and its efficiency was 93.1% for the SbFe and Sb_2Fe alloys. The first discharge capacity and charge capacity were 480mAh/g and 425mAh/g, and its efficiency was 88.5% for the Sb-Ge metal composite powder. The electric capacity gradually decreased with the charge-discharge cycle number increasing, and the discharge capacity and the charge capacity at 20th week corresponded to 70.6% and 73.7% of the initial discharge capacity and the charge capacity for the SbFe and Sb_2Fe alloys as anode material, and the discharge capacity and the charge capacity at 20th week corresponded to 78.1% and 82.4% of the initial discharge capacity and the charge capacity for the Sb-Ge metal composite powder as anode material. Although the initial electrochemical capacity and the charge/discharge efficiency for the SbFe and Sb_2Fe alloys were higher than those for the Sb-Ge metal composite powder, the irreversible capacity loss for the SbFe and Sb_2Fe alloys was bigger than that for the Sb-Ge metal composite powder as anode material. The reaction mechanism for SbFe and Sb_2Fe alloys or Sb-Ge composite powder with the Li was embedding/taking off lithium process. The SbFe and Sb_2Fe alloys or the Sb-Ge metal composite powder has certain embedded/taking off lithium ability, thus can be used as the candidate material for the lithium ion battery anode active material.

Introduction

Lithium ion battery has long cycle life, large energy density, high voltage and low self-discharge, good safety performance, no memory effect, pollution-free, etc.[1-3]. It is widely used in many fields. At present, the carbon materials are used commercially as lithium-ion battery anode materials. As anode materials of lithium ion battery, the carbon materials exist poor charge-discharge performance and larger energy loss [4]. The composite oxides and alloy as anode materials have high specific capacity, reversible lithium storage capacity and good conductivity compared with the carbon material. The solvent cannot be inserted and the fast charge-discharge ability is good when these materials are used as lithium ion battery anode materials [5-7].

Although the Sb single oxide electrochemical capacity is high, its cycle performance is poor. The Sb-based composite oxides were prepared by doping with other elements in single oxide. The cycle performance of the Sb-based composite oxides has been improved, but their irreversible capacity loss is bigger due to the bounded Li into "dead lithium" by the oxygen in active substances reacting with lithium to form LiO_2. Therefore, we want to remove oxygen in the composite oxide in order to reduce the irreversible capacity loss.

The Sb-base composite oxide $SbFeO_3$ and $SbGeO_{3.5}$ were prepared by coprecipitation, and then they were reduced by H_2 to obtain the alloys and the metal composite powder. The structure and
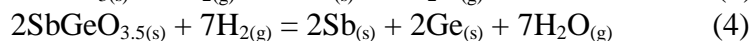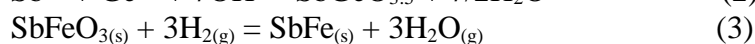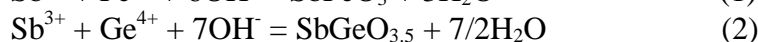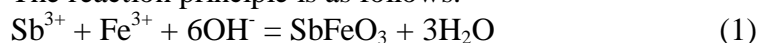
composition of the alloys and the metal composite powder were analyzed by the XRD, and the morphology of the alloys and the metal composite powder was observed by the SEM. The alloys or the metal composite powder was used as the anode material of lithium ion battery to prepare simulation lithium ion battery. The electrochemical performance of the simulation battery was characterized by using the constant current battery automatic tester.

Experimental

Preperation of alloy and composite powder. The $SbCl_3$ ethanol solution and the $FeCl_3 \cdot 6H_2O$ ethanol solution were uniformly added to ammonia at stirring and then heating reflux. The obtained products were thermally filtrated, and washed by distilled water to neutral, and then dried at 393 K for 48 h. The $SbFeO_3$ powder was obtained. The $SbGeO_{3.5}$ powder was also obtained by the same preparation way.

The $SbFeO_3$ powder was reduced by H_2 at 415°C for 4 h to obtain SbFe and Sb_2Fe alloys. The $SbGeO_{3.5}$ powder was reduced by H_2 at 580°C for 4 h to obtain Sb-Ge composite powder.

The reaction principle is as follows.

$$Sb^{3+} + Fe^{3+} + 6OH^- = SbFeO_3 + 3H_2O \qquad (1)$$
$$Sb^{3+} + Ge^{4+} + 7OH^- = SbGeO_{3.5} + 7/2H_2O \qquad (2)$$
$$SbFeO_{3(s)} + 3H_{2(g)} = SbFe_{(s)} + 3H_2O_{(g)} \qquad (3)$$
$$2SbGeO_{3.5(s)} + 7H_{2(g)} = 2Sb_{(s)} + 2Ge_{(s)} + 7H_2O_{(g)} \qquad (4)$$

Characterization of alloy and composite powder. The product phase was analyzed by using RINT-2200V/PC X-ray diffractometer (CuKa rayλ=1.054056Å). The voltage was 40kv, and the current was 40mA, and the scan range 20~800, and the scanning speed 80/min。

The product morphology was analyzed by JSM-6360LV type SEM.

The electrical property of the products was measured by automatic charging and discharging device.

Results and discussion

XRD analysis. The XRD spectra of samples were indicated in Fig. 1. Fig. 1 a was the $SbFeO_3$ sample no reduced, and b, c, d and e were the sample reduced by H_2 at 350°C, 395°C, 405°C,415°C, respectively. The results show that the structure of the $SbFeO_3$ was the amorphous due to no observe the obvious diffraction peak in Fig. 1 a. The diffraction peaks of the Fe_2O_3 were observed for the reduced sample $SbFeO_3$ at 350°C in Fig. 1 b. The diffraction peaks of the Sb_2O_3, Fe_3O_4, SbFe and Sb_2Fe were observed for the reduced sample $SbFeO_3$ at 395°C and 405°C in Fig. 1 c and d. The diffraction peaks of the SbFe and Sb_2Fe were observed only for the reduced sample $SbFeO_3$ at 415°C in Fig. 1 e. The diffraction peaks of the Fe_2O_3 disappeared, while the diffraction peaks of the Fe_3O_4, Sb_2O_3, SbFe and Sb_2Fe appeared for the reduced sample with reduction temperature rising to 395°C, and then the peak intensity of the Fe_3O_4 receded and the peak intensity of SbFe and Sb_2Fe enhanced for the reduced sample with the temperature increasing from 395°C to 415°C. These results indicate that $SbFeO_3$ reduction experienced from Fe_2O_3 to f Fe_3O_4 and Sb_2O_3, finally to form the SbFe and Sb_2Fe alloys.

Fig. 2 a was the $SbGeO_{3.5}$ sample no reduced, and b, c, d and e were the sample reduced by H_2 at 535°C, 550°C, 565°C, 580°C, respectively. The $SbGeO_{3.5}$ belonged to the crystal structure due to existing obvious sharp absorption peak in Fig. 2 a. The diffraction peaks of the GeO_2 were observed, meanwhile the diffraction peaks of the Sb and the Ge were observed also for the reduced sample $SbGeO_{3.5}$ at temperature reaching to 535°C, and then the peak intensity of the GeO_2 decreased gradually, the peak intensity of the Sb and the Ge increased gradually with the reduction temperature increasing from 535°C to 580°C. In the end, the peaks of the $SbGeO_{3.5}$ and GeO_2 disappeared thoroughly, the pears of the Sb and the Ge were observed only for the reduced sample at temperature 580°C. This shows that all $SbGeO_{3.5}$ was reduced completely to form metal Sb and Ge at reduction temperature 580°C. The separate diffraction peak of the Sb or Ge was observed, and the diffraction peak of the alloy was not observed. Therefore, the $SbGeO_{3.5}$ was reduced to obtain the Sb-Ge

composite powder instead of the alloy. It implies that the alloy could not be formed by the reducing the $SbGeO_{3.5}$ at 580°C.
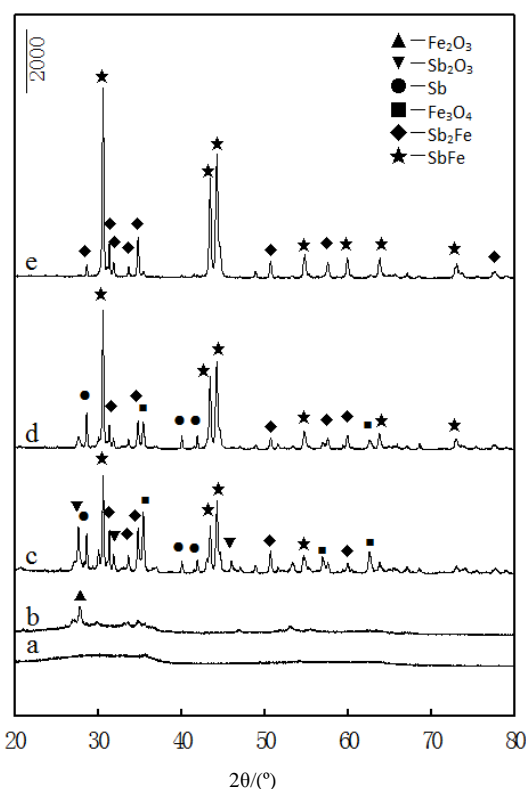

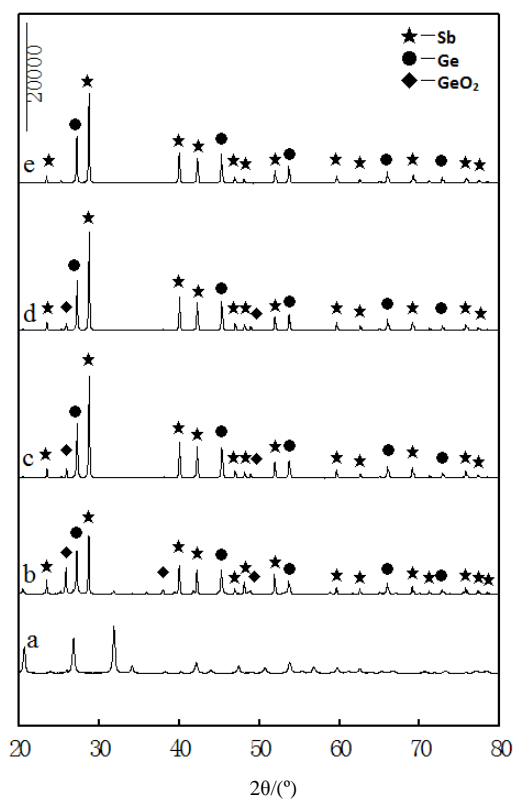Fig. 1. XRD patterns of samples reduced by H_2 (a. $SbFeO_3$, b. c. d. and e. reduced at 350°C, 395°C, 405°C, 415°C)

Fig. 2. XRD patterns of samples reduced by H_2 (a. $SbGeO_{3.5}$, b. c. d. and e. reduced at 535°C, 550°C, 565°C, 580°C)

SEM analysis. The morphology of the SbFe and Sb_2Fe alloys was characterized by the SEM. Fig. 3 is the SEM image of the the SbFe and Sb_2Fe alloys. The results indicate that alloy particles were uniform, and multiple particles formed a typical honeycomb mass of particles with obvious network structure. The average particle size of particles is about 100 nm.

Fig. 4 is morphology of the Sb-Ge composite powder characterized by the SEM. The results show that the particle distribution of the Sb-Ge metal composite powder were uniform, and presenting small ball shape, and gathered together to bigger ball shape. The average particle size of particles is about 100 nm.
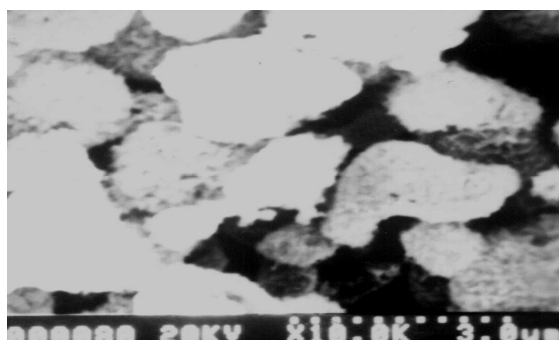

Fig. 3. SEM image of SbFe and Sb_2Fe alloy

Fig. 4. SEM image of Sb-Ge metal compound powde

Electrochemical properties. The charge and discharge curves of the simulation battery using the SbFe and Sb_2Fe alloys as lithium ion battery anode material were observed in Fig. 5. Table I was electrochemical properties of SbFe and Sb_2Fe alloys and Sb-Ge metal composite powder. The results indicate that the first discharge capacity (embedding lithium capacity) was 510mAh/g, the first charge capacity (taking off lithium capacity) was 475mAh/g, and its efficiency was 93.1%. In the first week of the discharge curve, there was the slope at higher voltage than 0.8 V, and no longer present at

following cycle. This was the decomposition reactions of SbFe surface oxide. Relative to the discharge platform at discharging curves 0.8 V, the corresponding charge platform could be seen at charging curve 1.1 V. This was typical of Li-Sb alloy reaction. The electric potential of reversible embedding lithium platform was 0.8V and 0.25V, and the corresponding electric potential of reversible taking off lithium platform was about 1.1V and 0.5V. After 20 cycles, its discharge capacity was 360 mAh/g, accounting for 70.6% of the initial discharge capacity, and charging capacity was 350 mAh/g, accounting for 73.7% of the initial charge capacity, and the efficiency was 97.2%. In SbFe and Sb_2Fe alloys, the Sb as active group (single active group) reacted with Li^+ to generate Li_ySb (y≤3).

Fig. 6 is charge and discharge curves of the simulation battery by the Sb-Ge metal composite powder as lithium ion battery anode material. Table I was electrochemical properties of SbFe and Sb_2Fe alloys and Sb-Ge metal composite powder. The results indicate that the first discharge capacity was 480mAh/g, the first charge capacity was 425mAh/g, and its efficiency was 88.5%. There were 2 obvious embedding lithium platform electric potential in the first week of discharge process at 0.75V and 0.2V, and its reversible taking off lithium platform electric potential was about 0.5V~1.1V. After 20 cycles, its discharge capacity was 375mAh/g, accounting for 78.1% of the initial discharge capacity, and charging capacity was 350 mAh/g, accounting for 82.4% of the initial charge capacity, and the efficiency was 93.3%. In Sb-Ge metal composite powder, both Sb and Ge as active group (double active group) reacted with Li^+ to generate Li_ySb (y≤3) and Li_xGe (x≤4.4).
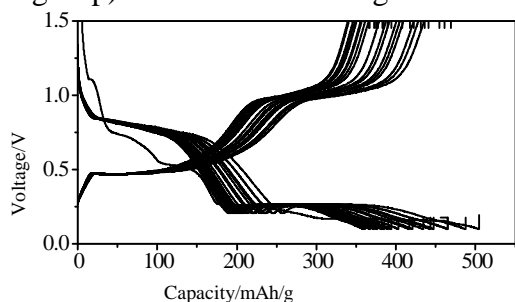

Fig. 5. Charge and discharge curves of the simulation battery for SbFe and Sb_2Fe alloy as lithium ion battery anode materials
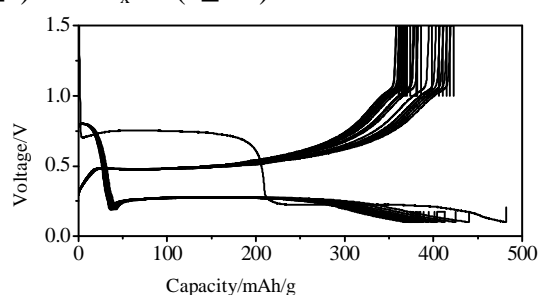

Fig. 6. Charge and discharge curves of the simulation battery for Sb-Ge composite powder as lithium ion battery anode materials

Table 1 Electrochemical properties of Sb-based Alloy and metal composite powder

Samples	First charge and discharge capacity （mAh/g）		Efficiency (%)
	Discharge	Charge	
Sb-Ge	480	425	88.5
SbFe Sb_2Fe	510	475	93.1
Samples	Charge and discharge capacity at 20th weeks （mAh/g）		Efficiency (%)
	Discharge	Charge	
Sb-Ge	375	350	93.3
SbFe Sb_2Fe	360	350	97.2

Conclusions

The Sb-based composite oxide ($SbFeO_3$, $SbGeO_{3.5}$) was prepared by coprecipitation method. The Sb-based composite oxide could be reduced smoothly by H_2 using self-designed closed loop system under low temperature. The reduction product of the $SbFeO_3$ was alloys (SbFe and Sb_2Fe), and the reduction product of the $SbGeO_{3.5}$ was the metal composite powder (Sb-Ge). The reduction reaction of the Sb-based composite oxide by H_2 in closed loop system generated easily, and the product particle size was smaller than 200nm.

The capacity gradually decreased with the charge-discharge cycle number increasing, and the discharge capacity at 20th week corresponded to 70.6% of the initial discharge capacity, and the charge capacity at 20th week corresponded to 73.7% of the initial charge capacity, and the charge/discharge efficiency was 97.2% after 20 cycles for the SbFe and Sb_2Fe alloys as lithium ion battery anode material. The capacity gradually decreased with the charge-discharge cycle number

increasing, and the discharge capacity at 20th week corresponded to 78.1% of the initial discharge capacity, and the charge capacity at 20th week corresponded to 82.4% of the initial charge capacity, and the charge/discharge efficiency was 93.3% after 20 cycles for the Sb-Ge metal composite powder as lithium ion battery anode material.

As lithium ion battery anode material, although the initial electrochemical capacity and the charge/discharge efficiency for the SbFe and Sb_2Fe alloys was higher than those for the Sb-Ge metal composite powder, the irreversible capacity loss for the SbFe and Sb_2Fe alloys was bigger than that for the Sb-Ge metal composite powder as lithium ion battery anode material.

The SbFe and Sb_2Fe alloys and Sb-Ge composite powder as active material of a lithium ion battery anode materials reacted with the lithium in the process of charging and discharging, and its reaction mechanism was embedding/taking off lithium reactions of the lithium with the metal by alloying/dealloying. The SbFe and Sb_2Fe alloys or the Sb-Ge metal composite powder has certain embedded/taking off lithium ability, thus can be used as the candidate material for the lithium ion battery anode active material.

Acknowledgment

References

[1] Y. Kubota, M. C. S. Escano, H.Nakanishi, et al. Journal of Alloys and Compounds 458 (2008) 151-157.

[2] J. Li, J. R. Dahn, J Electrochem Soc. 154 (2007) A156-A161.

[3] N. H.Zhao, L. C. Yang, P. Zhang, et al. Materials Letters 64 (2010) 972- 975.

[4] W. Qiu, G. Zhang, S. Lu, Q. Liu, Solid State Ionics 73 (1999) 121-125.

[5] X. Lou, C. Li, L. Archer, Advanced Materials 21 (2009) 2536-2539.

[6] J. T. Vaughey, L. Fransson, H. A. Swinger, et al. J. Power Sources 119-121 (2003) 64-68.

[7] Y. Hu, H. Zhang, H. Yang, J. Alloys Compd. 428 (2007) 327- 331.